DRAFT VERSION MAY 19, 2008
Preprint typeset using LaTeX style emulateapj v. 10/10/03

SLAC-PUB-13241

COMPARISON OF CLUSTER LENSING PROFILES WITH ΛCDM PREDICTIONS[1]

TOM BROADHURST[2], KEIICHI UMETSU[3,4], ELINOR MEDEZINSKI[2], MASAMUNE OGURI[5], YOEL REPHAELI[2,6]

Draft version May 19, 2008

ABSTRACT

We derive lens distortion and magnification profiles of four well known clusters observed with Subaru. Each cluster is very well fitted by the general form predicted for Cold Dark Matter (CDM) dominated halos, with good consistency found between the independent distortion and magnification measurements. The inferred level of mass concentration is surprisingly high, $8 < c_{\rm vir} < 15$ ($\langle c_{\rm vir}\rangle = 10.39 \pm 0.91$), compared to the relatively shallow profiles predicted by the ΛCDM model, $c_{\rm vir} = 5.06 \pm 1.10$ (for $\langle M_{\rm vir}\rangle = 1.25 \times 10^{15} M_{\odot}/h$). This represents a 4σ discrepancy, and includes the relatively modest effects of projection bias and profile evolution derived from N-body simulations, which oppose each other with little residual effect. In the context of CDM based cosmologies, this discrepancy implies some modification of the widely assumed spectrum of initial density perturbations, so clusters collapse earlier ($z \geq 1$) than predicted ($z < 0.5$) when the Universe was correspondingly denser.

Subject headings:

1. INTRODUCTION

Dark matter (DM) is understood to comprise $\simeq 85\%$ of the material Universe (Fukugita & Peebles 2004), in the form of massive halos around galaxies and clusters of galaxies. The density profile of a dark halo depends on the unknown nature of the DM and the way structure develops over cosmic time. Galaxy halos may be modified significantly when gas associated with the disk of a galaxy cools and condenses during its formation. In contrast, clusters are so massive that the virial temperature of the gas (typically, $3-15$ keV) is too high for efficient cooling and hence the cluster potential reflects the dominant DM.

Models for the development of structure now rest on accurate measurements of the power spectrum of mass fluctuations, the cosmological density of DM, and the contribution of a cosmological constant, Λ (Spergel et al. 2007; Komatsu et al. 2008). This framework is the standard "ΛCDM" cosmological model, with the added simple assumptions that DM is collisionless, reacts only gravitationally, was never relativistic ('Cold'), and with initially Gaussian-distributed density perturbations. In this context, detailed N-body simulations have established a clear prediction that CDM-dominated cluster halos should have relatively shallow, low-concentration mass profiles, where the logarithmic gradient flattens continuously toward the center with a central slope tending towards r^{-1}, interior to a characteristic radius, $r_s \lesssim 100-200{\rm kpc}/h$ (Navarro, Frenk, & White 1997, NFW, hereafter; Bullock et al. 2001; Hennawi et al. 2007; Neto et al. 2007; Duffy et al. 2008). This "NFW" profile is characterized by the (total) mass, $M_{\rm vir}$, within the virial radius, $r_{\rm vir}$, and by the concentration parameter, $c_{\rm vir} \equiv r_{\rm vir}/r_s$.

Interaction between clusters indicates DM is collisionless, in particular the "bullet cluster"(Markevitch et al. 2002) - where shocked gas lies between two substantial galaxy clusters, implying these clusters passed through each other recently (Markevitch et al. 2002). Here the weak lensing signal follows the bimodal distribution of member galaxies reflecting substantial DM associated with each cluster component (Clowe et al. 2006) and that this DM is relatively collisionless like the galaxies. These observations disfavour the class of alternative gravity theories for which the lensing signal is expected to trace the dominant baryonic contribution of the gas (Clowe et al. 2006). Other cases of interaction show that in general displacement of the gas relative to the DM is typically related to interaction (Jee et al. 2006; Okabe & Umetsu 2008).

For many clusters no obvious evidence of recent interaction is seen as the gas and member galaxies follow a symmetric, structureless distribution. Measurements of the mass profiles of these relaxed clusters may help in understanding the nature of DM, preferably relying on gravitational lensing signals where model-dependent assumptions are not required. For A1689, over 100 multiply-lensed images have been used to derive the inner mass profile(Broadhurst et al. 2005a), with the outer profile determined from weak lensing (Broadhurst et al. 2005b). Together, the full profile has the predicted NFW form, but with a surprisingly high concentration when compared to the shallow profiles of the standard ΛCDM model (Broadhurst et al. 2005b; Umetsu & Broadhurst 2008). Furthermore, good consistency is also found between the lensing based mass profile and the X-ray and dynamical structure of this cluster in model independent analyses (Lemze et al. 2007; Lemze et al. 2008, in preparation). A similar discrepancy is also indicated by lensing observations of other clusters e.g., MS2137-23 (Gavazzi et al. 2003) and CL0024+16 (Kneib et al. 2003).

Here we examine a sample of relaxed, high-mass clusters, to test the distinctive prediction of ΛCDM, and to settle empirically whether the mass profile of A1689 is unusual. In section §1 we describe the data reduction in §3 we present the weak lensing analysis and the magnification profiles derived from background number counts and make comparison with the prediction of the ΛCDM; in §4 we discuss our results and

[1] Based on data collected at Subaru Telescope, which is operated by the National Astronomical Observatory of Japan.

[2] School of Physics and Astronomy Tel Aviv University, Israel
[3] Institute of Astronomy and Astrophysics, Academia Sinica, P. O. Box 23-141, Taipei 106, Taiwan
[4] Leung Center for Cosmology and Particle Astrophysics, National Taiwan University, Taiwan
[5] Kavli Institute for Particle Astrophysics and Cosmology, Stanford University, 2575 Sand Hill Road, Menlo Park, CA 94025, USA
[6] Center for Astrophysics and Space Sciences, UC San Diego, California, USA

Submitted to Astrophysical Journal Letters

Work supported in part by US Department of Energy contract DE-AC02-76SF00515

conclusions.

2. DATA REDUCTION

We analyse deep images of A1689, A1703, A370, RXJ1347-11 taken by the wide-field camera Suprime-Cam ($34\prime \times 27\prime$, Miyazaki et al. 2002) in Subaru (8.3m) which are observed deeply in several optical passbands, listed in Table 1. These clusters are of interest due to the exceptional quality of the data, with exposures in the range 2000s-10000s per pass band, with seeing ranging from $0''.5$ to $0''.75$. We use either R or I bands for our weak lensing measurements (described below §3) for which the instrumental response, sky background and seeing conspire to provide the best images. All the available bands are used to define colours with which we separate cluster members from the background in order to minimise dilution of the weak lensing signal by unlensed objects.

The standard pipeline reduction software for Suprime-Cam (Yagi et al. 2002) is applied for flat-fielding, instrumental distortion correction, differential refraction, PSF matching, sky subtraction and stacking. Photometric catalogs are constructed from stacked and matched images using Sextractor (Bertin & Arnaut 1996). We select red galaxies with colours redder than the colour-magnitude sequence of cluster E/SO galaxies. The sequence forms a well defined line due to the richness and relatively low redshifts of our clusters. These red galaxies are expected to lie in the background by virtue of k-corrections which are greater than for the red cluster sequence galaxies. We also include very blue galaxies falling far from the cluster sequence,$> 1.^m5 - 2.^m5$, depending on the passbands available for each cluster (listed in Table 1), to minimise cluster contamination (see Medzinski et al. 2007). Typically the proportion of blue galaxies used is around 50% of the red background. In addition, we adopt a conservative magnitude limit of $m < 25.5 - 26.0$, depending on the depth of the data for each cluster, to avoid incompleteness.

3. MEASUREMENTS OF LENSING EFFECTS

These data permit high quality weak lensing measurements, following established methods required to deal with instrumental and atmospheric effects following the formalism outlined in Kaiser, Squires, & Broadhurst (1995), with modifications described in Erben et al. (2001). Full details are presented in Umetsu & Broadhurst (2008). Figure 1 shows the gravitational shear field by locally averaging the corrected distortions of colour-selected background galaxies of each cluster. This is compared to the distribution of color-selected cluster sequence galaxies. In each case, one large symmetric cluster is visible around which the lensing distortion pattern is clearly tangential, with little significant substructure. The derived radial profiles of the lensing distortion are seen to be very similar in form (left panel of Figure 2), with differing amplitudes reflecting a range of mass. Importantly the B-mode lensing signal of each cluster (lower panel of Figure 2a) shows no significant signal implying consistent no significant assymetry.

The NFW profile fits well each cluster (Figure 2; Table 1), but surprisingly the derived concentrations lie well in excess of the standard ΛCDM model (Figure 3). For the derived masses of our clusters, the predicted mean concentration is $c_{\rm vir} \sim 5.06 \pm 1.1$ based on Duffy et al. (2007) using the improved WMAP5 (Komatsu et al. 2008). Our best-fitting values instead range over $8 < c_{\rm vir} < 15$, with a mean value of ($\langle c_{\rm vir} \rangle = 10.39 \pm 0.91$) representing a 4.8σ discrepancy. Our measurements also imply A370 is the most massive cluster

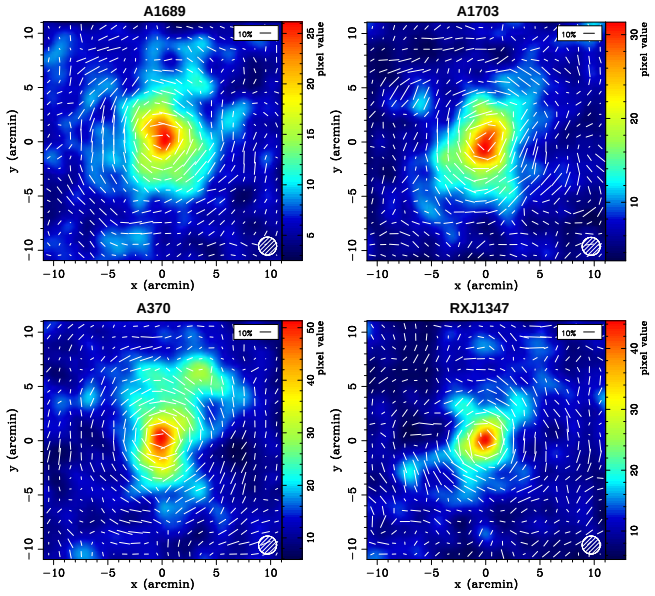

FIG. 1.— Maps of the surface number-density distribution of color-selected cluster member galaxies, with the gravitational shear of background galaxies overlayed; 10% ellipticity is indicated top right, and the resolution of the distortion map is shown bottom right. In each case a single concentration of galaxies is visible, around which a coherent tangential pattern is centered, with little significant substructure.

now known, $M_{\rm vir} = 2.93 \times 10^{15} M_\odot / h_{70}$, with a virial mass twice that of RXJ1347-11, the most X-ray luminous cluster known.

Note, when model fitting an estimate of the background depth is required. The mean depth is sufficient for our purposes as the variation of the lens distance ratio, D_{ds}/D_s, is slow for our sample because the clusters are at relatively low redshift compared to the redshift range of the background galaxies. The estimated mean depth of the combined red+blue background galaxies is listed in column 5, which we obtain by applying our colour-magnitude selection to Subaru imaging of the HDF region (Capak et al. 2004), where photometric redshifts are reliable for red galaxies, with a mean redshift close to $z = 1.2$ depending on the details of the colour magnitude selection. For the blue galaxies we may rely on the zCOSMOS deep redshift survey (Lilly et al. 2008) where our mean depth is typically $z \simeq 2.1$.

Lensing measures projected mass and so a statistical bias arises from the triaxiality of clusters in cases where the long axis lies along the line-of-sight. This leads to an $\sim 18\%$ increase in the mean value of lensing derived concentrations based on ΛCDM (Oguri et al. 2005; Hennawi et al. 2007), and an overall discrepancy in $c_{\rm vir}$ of 4.0σ with respect to the predictions. A larger bias is inferred for clusters selected by the presence of large arcs, $\sim 34\%$, representing the most triaxial cases (Hennawi et al. 2007). Our sample is defined by the quality of available imaging and includes clusters observed for reasons other than lensing, hence it is unlikely that these clusters are all particularly triaxial with the long axes pointing to the observer. Even so, applying the maximum estimated bias ($\sim 50\%$, Oguri & Blandford, in preparation) cannot account for our measurements (Figure 3).

Multiply-lensed images are visible in all our clusters, from which the inner mass distribution may be determined (Broadhurst et al. 2005a; Halkola et al. 2008; Hennawi et al.

TABLE 1. THE SUBARU DISTORTION MEASUREMENTS COMBINED WITH THE EINSTEIN-RADIUS CONSTRAINT.

Cluster Name	z	Subaru filters	Einstein Radius (") (′′)	$\langle D_{ds}/D_s \rangle$	$M_{\rm vir}$ $(10^{15} M_\odot/h_{70})$	$c_{\rm vir}$	χ^2/dof
A1689	0.183	$V_J i'$	52 ($z_s = 3.05$)	0.704	$1.59^{+0.24}_{-0.22}$	$15.69^{+3.96}_{-2.88}$	4.94/9
A1703	0.258	$g'r'i'$	33 ($z_s = 2.8$)	0.722	$1.30^{+0.24}_{-0.20}$	$9.92^{+2.39}_{-1.63}$	2.69/5
A370	0.375	$BR_C z'$	43 ($z_s = 1.5$)	0.606	$2.93^{+0.36}_{-0.32}$	$7.75^{+1.12}_{-0.92}$	5.54/8
RX J1347-11	0.451	$V_J R_C z'$	35 ($z_s = 1.8$)	0.553	$1.47^{+0.26}_{-0.23}$	$10.42^{+3.25}_{-2.13}$	6.25/7

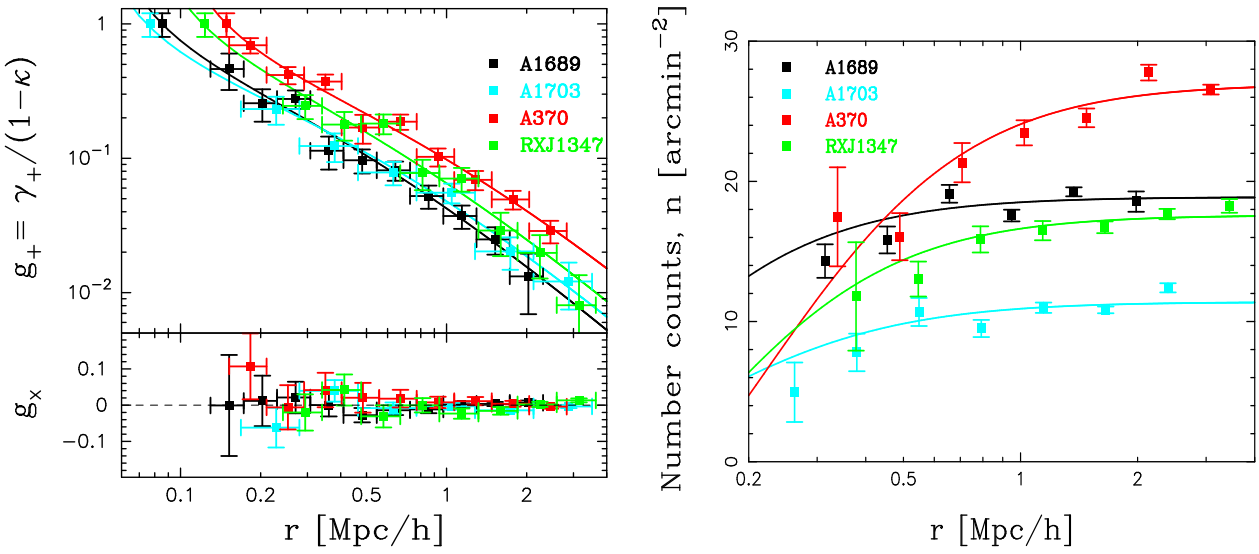

FIG. 2.— (*Left*): Tangential distortion profiles of the 4 clusters based on the combined red and blue background samples and compared with the best-fitting NFW model. The Einstein-radius determined from multiply-lensed images is indicated, marking the point of maximum distortion, $g_+ = 1$. Shown below is the rotated shear, $g_\times$, demonstrating no obvious non-tangential distortion. (*Right*): Profiles of background red galaxy counts, whose intrinsic slope is relatively shallow, so lens magnification reduces the observed numbers towards the center. Over-plotted are normalised NFW models derived from the distortion profiles in the left panel, demonstrating consistency between these two independent lensing observables; note A370 is shifted upward 40% for clarity. The count uncertainty is obtained by sub-dividing each annulus into equal area cells, with a tail of $> 2\sigma$ cells excluded to remove inherent small scale clustering of the background. Small areas around each bright object ($m_R < 21$) are excluded, including cluster members, interior to 3 times the isophotal radius, where the detection of faint galaxies is significantly compromised (Broadhurst et al. 2005b; Umetsu & Broadhurst 2008).

2008) and an equivalent Einstein radius derived by averaging azimuthally (Figure 2) which for most cases is close to the observed radius. For A370 the critical curves are significantly elongated, and although the mass distribution is generally rounder in shape than the critical curves, there is clearly an influence of substructure visible in the distribution of the arcs and clumpy X-ray emission in the inner region, $< 1'$, (e.g. Shu et al. 2008), beyond which the lensing pattern and galaxy distribution is more symmetric as seen in Figure 1. For each cluster the NFW parameters derived with or without the Einstein radius constraint are found to be closely consistent and in combination they are more precisely determined - see Table 1.

We also examine the magnification profile, $\mu(r)$, via the surface number density of background galaxies (Broadhurst, Taylor, & Peacock 1995). At faint fluxes where the counts follow a power-law slope, $s = d\log N(<m)/dm$, lensing modifies the true density, $N_0(m < m_{\rm lim})$, by, $N(< m_{\rm lim}) = N_0(< m_{\rm lim})\mu(r)^{2.5s-1}$, implying competition between the magnified sky, which reduces the surface density, and an increase of galaxies magnified above the flux limit. Here we use only galaxies lying redward of the cluster sequence because for these the intrinsic count-slope of faint red galaxies is relatively flat, $s \sim 0.1$, so a net count depletion results, which we readily detect for each cluster, increasing towards the center (Figure 2). In each case the observed count profile is consistent with the best fitting NFW profile derived from the distortion measurement (Figure 2, right panel, with same colour code), considerably strengthening our conclusions, and also establishing very clearly the utility of the background red galaxies for measuring magnification in deep images. Note, the variation in the total number of background counts seen in Figure 2 simply reflects the relative depth of the imaging data and also to some extent the redshift of the cluster, which lies redder in colour space with increasing cluster redshift, thereby reducing the numbers of background galaxies which can be selected to lie redward of the sequence for our purposes.

4. DISCUSSION

We have shown that the mass distribution of a sample of the most massive clusters foolow a very similar form in terms of the observed lensing based profiles. The distortion profiles measured are amongst the most accurate constructed to date and the great depth of the Subaru imaging permits magnification profiles to be established with unprecedented detail using the background red galaxy counts. The magnification

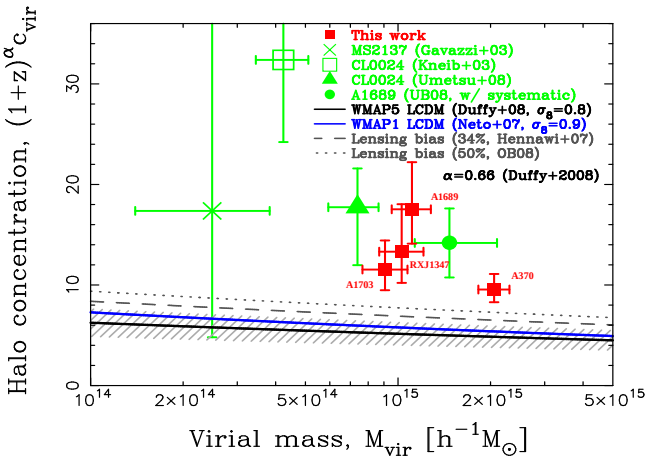

FIG. 3.— Comparison of observations with the ΛCDM model, based on N-body simulations for the $c_{\rm vir}-M_{\rm vir}$ relation, derived at $z=0$. The predictions of Duffy et al. (2008) ($\sigma_8=0.8$, WMAP5) and Neto et al. (2007) ($\sigma_8=0.9$, WMAP1) are shown as solid curves, with 1σ uncertainty (from Neto et al. 2007) indicated by the hatched area. Also shown is the level of selection and orientation bias for projected masses based on ΛCDM (dashed curves, see text). The data points are all derived from lensing alone, and are multiplied by $(1+z)^{0.66}$ at the cluster redshift, for consistency with the evolution of $c_{\rm vir}(M_{\rm vir})$ derived from ΛCDM simulations by Duffy et al. 2008. Note, a significant correction for substructure is required for Cl0024+16 (Umetsu et al., in preparation). Clearly the data lie well above the predicted relation even when possible sources of bias are considered.

and distortion profiles are fitted well by the general NFW profile for CDM dominated halos, which continuously steepens with radius, but the profiles derived are more concentrated than predicted by ΛCDM based simulations for which clusters of $\sim 10^{15}M_{\odot}$, form late ($z<0.5$) with low concentrations, reflecting the low mean cosmological mass density today.

Tension with the standard ΛCDM model is also indicated by the observed Einstein radii of very massive clusters, including those studied here, which lie well beyond the predicted range derived from massive halos generated in ΛCDM based simulations (Broadhurst & Barkana 2008). In addition, a significant discrepancy is also claimed for X-ray derived cluster concentrations, with respect to the ΛCDM based on WMAP5 parameters (Duffy et al. 2008).

Without resorting to radical proposals regarding the nature of DM, our findings imply the central region of clusters collapsed earlier than expected. Assuming the simple redshift relation $c_{\rm vir}(z)=c_0(1+z)$ (e.g., Wechsler et al. 2006), relating central cluster densities to the cosmological mean density, then the formation of clusters with $c_{\rm vir}(1+z)=10-15$ corresponds to $z\geq 1$, significantly earlier than in the standard ΛCDM, for which clusters form today with $c_0\sim 5.6$.

The presence of massive clusters at high redshift ($z\sim 2$), and the old ages of their member galaxies (Zirm et al. 2008; Blakeslee et al. 2003), may also imply clusters collapsed at relatively early times(Mathis, Diego, & Silk 2004), for which accelerated growth factors have been proposed, adopting a generalised equation of state (Sadeh & Rephaeli 2008). Alternatively, since clusters correspond to rare density maxima, then any non-Gaussianity in the early fluctuation spectrum may advance cluster formation (Matthis, Diego, & Silk 2004; Sadeh, Rephaeli, & Silk 2007). Our results present a challenge to some of these models, since earlier cluster formation must not also enhance significantly the abundance of clusters.

Acknowledgements: This work is in part supported by the Israeli Science Foundation and the National Science Council of Taiwan under the grant NSC95-2112-M-001-074-MY2 and by the US Department of Energy, contract DE-AC02-76SF00515.

REFERENCES

Bertin, E., & Arnouts, S. 1996, A&AS, 117, 393
Blakeslee, J. P., et al. 2003, ApJL, 596, L143
Broadhurst, T. J., Taylor, A. N., Peacock, J. A., 1995, ApJ, 438, 49
Broadhurst, T., et al. 2005a, ApJ, 621, 53
Broadhurst, T., Takada, M., Umetsu, K. et al. 2005b, ApJL, 619, L143
Broadhurst,T.J.& Barkana R., 2008, MNRAS, submitted.
Capak, P., et al. 2004, AJ, 127, 180
Clowe, D., et al, 2006, ApJL, 648, L109
Bullock, J, et al, 2001, MNRAS, 321, 559
Duffy, A.R., Schaye, J., Kay, S.T., Della Vecchia, C. 2008, MNRAS, submitted
Erben, T., Van Waerbeke, L., Bertin, E., Mellier, Y., Schneider, P., 2001, A&A, 366, 717
Fukugita & Peebles 2004, ApJ, 616, 643
Gavazzi, R., Fort, B., Mellier, Y., Pelló, R., & Dantel-Fort, M. 2003, A&A, 403, 11
Halkola, A., et al. 2008, A&A, 481, 65
Hennawi, J. F., Dalal, N., Bode, P., & Ostriker, J. P. 2007, ApJ, 654, 714
Hennawi, J. F., et al. 2008, AJ, 135, 664
Jee, M. J., White, R. L., Benítez, N., Ford, H. C., Blakeslee, J. P., Rosati, P., Demarco, R., & Illingworth, G. D. 2005, ApJ, 618, 46
Kaiser, N., Squires, G., Broadhurst, T., 1995, ApJ, 449, 460
Kneib, J.-P. et al. 2003, ApJ, 598, 804
Komatsu, E., et al. 2008, ApJS, submitted.
Lemze, D., Barkana, R., Broadhurst, T. J., & Rephaeli, Y. 2008, MNRAS, 386, 1092
Lilly, S. J., et al. 2007, ApJS, 172, 70
Markevitch, M., et al, 2002, ApJL, 567, L27
Mathis, H., Diego, J. M., & Silk, J. 2004, MNRAS, 353, 681
Medezinski, E., et al. 2007, ApJ, 663, 717
Miyazaki, S., et al. 2002, PASJ, 54, 833
Navarro, J. F., Frenk, C. S., White, S. D. M., 1997, ApJ, 490, 493
Neto, A.F. et al. 2007, MNRAS, 381, 1450
Oguri, M., Takada, M., Umetsu, K., & Broadhurst, T. 2005, ApJ, 632, 841
Okabe, N., Umetsu, K. 2008, PASJ 60,345 (arXiv:astro-ph/0702649)
Sadeh, S., & Rephaeli, Y. 2008, MNRAS, submitted.
Sadeh, S., Rephaeli, Y., & Silk, J. 2007, MNRAS, 380, 637
Shu, C., Zhou, B., Bartelmann, M., Comerford, J. M., Huang, J. -., & Mellier, Y. 2008, ArXiv e-prints, 805, arXiv:0805.1148
Spergel, D. N. et al. 2007, ApJS, 170, 377
Springel et al. 2005, Nature, 435, 629
Umetsu, K. & Broadhurst, T. 2008, ApJ in press (arXiv:astro-ph/0712.3441)
Wechsler, R., Zentner, A., Bullock, J. S., Kravtsov, A. V., & Allgood, B. 2006, ApJ, 652, 71
Yagi, M., Kashikawa, N., Sekiguchi, M., et al. 2002, AJ, 123, 66
Zirm, A.,W., et al. 2008, ApJ, 679,2